





Original Research

Antagonistic Relationship of Interferon-Inducible Protein 10 and Lipoxin A4 in HTR-8-SVneo Cells: A Pilot Study

Jianfang Wang^{1,*}, Chunxiao Fang¹, Limei Quan¹, Yi Zhou¹¹Department of Obstetrics, Jinhua People's Hospital, 321000 Jinhua, Zhejiang, China*Correspondence: jefayeking@163.com (Jianfang Wang)

Academic Editor: Paolo Ivo Cavoretto

Submitted: 31 July 2025 Revised: 20 October 2025 Accepted: 31 October 2025 Published: 25 December 2025

Abstract

Background: Proper invasion and growth of trophoblast cells are crucial for the prevention of preeclampsia. This pilot study, conducted with a small sample size, focused on the regulatory effects of interferon-inducible protein 10 (IP-10) and lipoxin A4 (LXA4) on HTR-8-SVneo trophoblast cells. **Methods:** A total of 5 patients with preeclampsia and 5 normotensive pregnant women were enrolled in this study. Serum and placental levels of IP-10, LXA4, and the LXA4 receptor (ALX) were measured. Both IP-10 and ALX were silenced in HTR-8-SVneo cells. The effects on HTR-8-SVneo cell behaviors were assessed using wound healing assay, transwell assay, colony formation assay, Cell Counting Kit-8 (CCK8) assay, flow cytometry, and terminal deoxynucleotidyl transferase deoxyuridine triphosphate nick-end labeling (TUNEL) staining. Inflammatory and oxidative stress markers were measured using biochemical assay. Apoptosis-related proteins were measured via western blotting. **Results:** High levels of IP-10 and low levels of LXA4, accompanied by decreased ALX expression, were observed in patients with preeclampsia. IP-10 knockdown significantly stimulated the invasion, migration and proliferation of HTR-8-SVneo cells while inhibiting apoptosis, whereas ALX silencing exerted the opposite effects. Silencing of IP-10 or ALX also produced opposing effects on the regulation of oxidative stress and inflammation in HTR-8-SVneo cells. **Conclusions:** Although this pilot study has a small sample size (n = 5 per group) and inherent limitations, it provides noteworthy preliminary evidence of an antagonistic relationship between IP-10 and LXA4 in HTR-8-SVneo cells.

Keywords: preeclampsia; interferon-inducible protein 10; lipoxin A4; HTR-8-SVneo cell

1. Introduction

Preeclampsia is a pregnancy-specific disorder that typically develops after the 20th week of gestation. It is clinically characterized by proteinuria and hypertension [3]. It causes multi-organ impairment, being a leading cause of maternal mortality, and may also result in placental abruption, fetal growth restriction, and perinatal deaths [4,5]. While the exact etiology of preeclampsia remains unclear, defective spiral artery remodeling is widely recognized as a key pathogenic factor [6]. Appropriate trophoblast invasion and growth are crucial for spiral artery remodeling and placenta development [7]. Consequently, factors inducing trophoblast dysfunction may trigger abnormal placental formation, providing new insights into preeclampsia pathogenesis.

Interferon-inducible protein 10 (IP-10) is a Cys-X-Cys (CXC; X means any amino acid) chemokine produced by activated fibroblasts, monocytes, endothelial cells, and lymphocytes [8], playing a significant biological role in mediating Th1-type inflammatory responses and inhibiting angiogenesis. Clinical studies have identified elevated levels of IP-10 in patients with various diseases characterized by Th1-dominant inflammatory reactions, such as pulmonary tuberculosis, systemic lupus erythematosus, rheumatoid arthritis, and atherosclerosis [9–12]. These conditions elicit the corresponding immune responses. Notably, serum IP-

10 levels are significantly higher in pregnant women with preeclampsia than in those without [13,14], suggesting a potential association between IP-10 and preeclampsia onset. Lipoxin A4 (LXA4), produced via dual lipoxygenase-mediated lipoxygenation of arachidonic acid, serves as a ‘stop signal’ in inflammation-related diseases [15]. Its primary receptor is formyl peptide receptor 2, also referred to as the LXA4 receptor (ALX). Studies have demonstrated that LXA4 effectively reduces the production of tumor necrosis factor- α (TNF- α), interleukin-1 beta (IL-1 β), and reactive oxygen species (ROS) in lung tissues in acute lung injury [16,17]. This promotes the resolution of inflammation and alleviates oxidative stress damage, thereby inhibiting the progression of pneumonia. More importantly, LXA4 deficiency is strongly associated with severe preeclampsia in a rat model [18]. However, the regulatory mechanisms of IP-10 and LXA4 in preeclampsia remain not fully clarified.

This pilot study investigated the role of IP-10 and LXA4 in preeclampsia progression using *in vitro* models. They exhibited antagonistic effects on the proliferation, migration, and invasion capabilities of HTR-8-SVneo cells. Our findings suggest that molecular-targeted agents enhancing LXA4 levels or inhibiting IP-10 levels may facilitate proper trophoblast invasion and growth, thereby reducing preeclampsia risk.



Table 1. The baseline data of pregnant women.

| Baseline characteristics | Normal (n = 5) | Preeclampsia (n = 5) | p-value |
|---------------------------------|----------------|----------------------|---------|
| Maternal age (years) | 30.8 ± 2.3 | 31.2 ± 2.5 | 0.78 |
| Gestational age (weeks) | 37.1 ± 0.9 | 36.5 ± 1.2 | 0.42 |
| Diastolic blood pressure (mmHg) | 72.0 ± 4.1 | 95.0 ± 6.2 | <0.001 |
| Systolic blood pressure (mmHg) | 118.0 ± 5.3 | 152.0 ± 8.5 | <0.001 |
| 24-hour urine protein (g) | 0.12 ± 0.05 | 1.80 ± 0.60 | <0.001 |

2. Materials and Methods

2.1 Patients

Five pregnant women with preeclampsia who underwent cesarean section at Jinhua People's Hospital were enrolled. Venous blood samples (5 mL) were obtained via venipuncture and centrifuged at 3000 revolutions per minute for 10 min to obtain serum. Placental tissues were collected within 60 min after cesarean delivery, immediately frozen in liquid nitrogen, and kept at -80°C for subsequent analysis. Preeclampsia was diagnosed based on the following criteria: (i) after 20 weeks of gestation, the diastolic (≥ 90 mmHg) and/or systolic blood pressure (≥ 140 mmHg) readings were in an abnormal state; (ii) proteinuria level ≥ 0.3 g per day. The normal group (n = 5) was matched with the preeclampsia group by maternal age and gestational week. Individuals with the following complications were excluded from both groups, including renal diseases, primary hypertension, gestational diabetes, alcoholism, smoking, fetal congenital abnormalities and twin pregnancy. All participants gave their written informed consent. The Ethics Committee of Jinhua People's Hospital granted ethical approvals for this study (approval number: 2023-007). This study adhered to the ethical guidelines outlined in the Declaration of Helsinki. Baseline characteristics of participants are presented in Table 1.

2.2 Cell Culture, Hypoxia Stimulation and Transfection

The human immortalized HTR-8-SVneo trophoblast cell line (cat.no. CL-0765), obtained from Pricella Biotechnology (Wuhan, Hubei, China), was maintained in a specialized medium (cat.no. CM-0765; Pricella Biotechnology). The cells tested negative for the presence of mycoplasma and were authenticated by short tandem repeat profiling. Cells in the control group were cultured under standard normoxic conditions (37°C , 5% CO_2). For hypoxia treatment, cells were exposed to an atmosphere of 93% N_2 , 2% O_2 , and 5% CO_2 [19,20].

HTR-8-SVneo cells (1×10^4 cells per well) were cultured until they reached 90% confluence in 6-well plates. Subsequently, short interfering (siRNA) targeting IP-10 (si-IP-10-1/-2/-3), si-ALX-1/-2/-3 or the negative control (si-NC) (Genomeditech, Shanghai, China) were transfected into HTR-8-SVneo cells for 48 h using GMTrans Liposomal Transfection Reagent (Genomeditech, Shanghai, China). Finally, HTR-8-SVneo cells were collected to detect transfection efficiency through quantitative real-

time polymerase chain reaction (qRT-PCR). The relative mRNA expression levels of IP-10/ALX were determined using the $2^{-\Delta\Delta\text{Ct}}$ method, with si-NC as the negative control. "Highly efficient silencing" was defined as a reduction in mRNA expression of $\geq 60\%$ compared to the si-NC group. Experiments were conducted in triplicate and repeated three times.

2.3 qRT-PCR

HTR-8-SVneo cells and placental tissues were collected for RNA isolation via a Total RNA extraction Kit (cat.no. RE-03011; Foregene Biotechnology, Chengdu, Sichuan, China). cDNA was then synthesized with the Seq-Hunt® First Strand cDNA Synthesis Kit (cat.no. CA01; Seq-Hunt Biotechnology, Beijing, China). PCR analysis was performed on a Real-time PCR System (version 1.4.1; Applied Biosystems, Foster City, CA, USA) using $2 \times$ Blue Universal SYBR qPCR Master Mix (cat.no. AF07; Seq-Hunt Biotechnology) per the manufacturer's instructions. Relative expression was calculated via the $2^{-\Delta\Delta\text{Ct}}$ values method, with glyceraldehyde-3-phosphate dehydrogenase (GAPDH) as the reference gene for normalization. Table 2 provided a list of gene primers used in this research. Experiments were conducted in triplicate and repeated three times. Clinical results were performed with five human samples per group.

2.4 Western Blot Assay

Protein extracts from HTR-8-SVneo cells and placental tissues were extracted using radioimmunoprecipitation assay (RIPA) lysis buffer (cat.no. BL504A; Biosharp Life Sciences, Hefei, Anhui, China). Subsequently, the protein samples were separated by SDS-PAGE and transferred onto a Polyvinylidene Fluoride (PVDF) membrane. Subsequently, the membrane was incubated with 5% non-fat milk (cat.no. BS102; Biosharp Life Sciences) at room temperature for 1 h to block any non-specific binding sites. The membrane was probed with primary antibodies against IP-10 (cat.no. 10937-1-AP; 1:200; Proteintech, Wuhan, Hubei, China), ALX (cat.no. bs-23765R; 1:1000; Bioss Biotechnology, Beijing, China), B-cell lymphoma 2 (Bcl-2) (cat.no. ABP50759; 1:1000; Abbkine Scientific, Wuhan, Hubei, China), B-cell lymphoma 2-associated X protein (Bax) (cat.no. 60267-1-Ig; 1:10,000; Proteintech), Caspase-3 (cat.no. ab32351; 1:5000; Abcam, Cambridge, UK) and GAPDH (cat.no. 60004-1-Ig; 1:50,000; Proteintech) at 4°C overnight. After three washes with

Table 2. Real-time PCR Primer synthesis list.

| Gene | | Sequences |
|---------------|---------|-----------------------------------|
| IP-10 | Forward | 5'- TCTGAGCCTACAGCAGAGGA -3' |
| | Reverse | 5'- ATGCAGGTACAGCGTACAGTT -3' |
| ALX | Forward | 5'- AAGCCAAGAAGCACACAGGA -3' |
| | Reverse | 5'- CAATGGGAGGATCCGCAGAA -3' |
| Bcl-2 | Forward | 5'- AAAAATACAACATCACAGAGGAAGT -3' |
| | Reverse | 5'- GTTTCCCCCTTGGCATGAGA -3' |
| Bax | Forward | 5'- GAGCAGCCCAGAGGCG -3' |
| | Reverse | 5'- TGAGACACTCGCTCAGCTTC -3' |
| Caspase-3 | Forward | 5'- TCCTAGCGGATGGGTGCTAT -3' |
| | Reverse | 5'- CTCACGGCCTGGGATTCAA -3' |
| TNF- α | Forward | 5'- GACAAGCCTGTAGCCCATGT -3' |
| | Reverse | 5'- GGAGGTTGACCTTGGTCTGG -3' |
| IL-1 β | Forward | 5'- AACCTCTCGAGGCACAAGG -3' |
| | Reverse | 5'- AGATTCGTAGCTGGATGCCG -3' |
| GAPDH | Forward | 5'- AAGGTCATCCCTGAGCTGAAC -3' |
| | Reverse | 5'- ACGCCTGCTTACCACCTTCT -3' |

IP-10, interferon-inducible protein 10; ALX, LXA4 receptor; TNF- α , tumor necrosis factor-alpha; IL-1 β , interleukin-1 beta; Bcl-2, B-cell lymphoma 2; Bax, B-cell lymphoma 2-associated X protein; GAPDH, glyceraldehyde-3-phosphate dehydrogenase.

Tris-buffered saline with Tween 20 (TBST, 0.1% Tween 20) for 10 min each, the membrane was further incubated with secondary antibodies (cat.no. A21020 & A21010; 1:10,000; Abbkine Scientific) at 25 °C for 2 h. Protein signals were detected using a SuperKine™ ECL Kit (cat.no. BMU101-CN; Abbkine Scientific), and analyzed with Image Tool software (version 3.0; UTHSCSA, San Antonio, TX, USA). Relative protein expression levels were normalized to GAPDH. Experiments were conducted in triplicate and repeated three times. Clinical results were performed with three human samples per group.

2.5 Immunohistochemistry

Placental tissues were fixed, paraffin-embedded, deparaffinized, and rehydrated. After antigen retrieval, tissue sections were incubated overnight at 4 °C with primary antibodies IP-10 (1:200; Proteintech), CXC motif chemokine receptor 3 (CXCR3) (1:200; Proteintech) and ALX (1:1000; Bioss Biotechnology). This was followed by a subsequent incubation step using horseradish peroxidase-conjugated secondary antibody (1:3000; Abbkine Scientific) for 1 h at 37 °C. After that, each slice was stained with 3,3'-diaminobenzidine (DAB), and then counterstained with hematoxylin for 1 min. The sections were differentiated with 1% hydrochloric acid ethanol for 30 sec, followed by bluing in 0.5% ammonia water for 1 min. After dehydration through a graded ethanol series and clearing with xylene, the slices were mounted. Microscopic imaging was performed under a light microscope (YONGXIN OPTICS, Ningbo, Zhejiang, China). Clinical results were performed with three human samples per group.

2.6 Measurement for HTR-8-SVneo Cell Proliferation

Colony formation assay was performed to assess the proliferative potential. Briefly, HTR-8-SVneo cells, with a density of 1×10^3 cells per well, were seeded into 6-well culture plates for one week. Cells were then washed with PBS, fixed with 4% paraformaldehyde, and stained with 0.1% crystal violet for 15 min. Colonies were counted under a light microscope (Olympus, Tokyo, Japan) and analyzed with ImageJ software (version 2.0; National Institutes of Health, Bethesda, MD, USA). Experiments were conducted in triplicate and repeated three times.

For the measurement of cell viability, HTR-8-SVneo cells with the density of 3×10^3 cells/mL were seeded in 96-well plates and cultured for 48 h. After that, 10 μ L CCK-8 solution (cat.no. CK04; DOJINDO LABORATORIES, Shanghai, China) was added to each well, followed by 2 h of incubation. HTR-8-SVneo cell viability was measured under a microplate reader (Bio-Rad Laboratories, Hercules, CA, USA), where optical density measurements were recorded at a wavelength of 450 nm. Experiments were conducted in triplicate and repeated three times.

2.7 Transwell Assay

Briefly, 100 μ L of Matrigel (1:8 diluted in serum-free medium) was uniformly spread onto the polycarbonate membrane surface in upper chamber, and then incubated at 37 °C for 30 min to allow gelation. Complete medium (containing 10% fetal bovine serum) was added to the lower chamber of the 24-well plates, and the transwell chamber was placed in the 24-well plates with tweezers. In the upper chamber, a total of 2×10^5 HTR-8-SVneo cells was added, and further cultured in an incubator for 24 h. After removing the chamber, Matrigel and non-invading cells in the upper chamber were gently removed. Subsequently, 4% paraformaldehyde was added to a new 24-well plate and fixed for 30 min. Then, 0.1% crystal violet was used to stain the invaded cells for 5 min. After cleaning with PBS for 3 times, the remaining crystal violet was removed, and the upper side of the chamber was wiped with a cotton swab. After air drying, five random fields were selected under a high-power microscope (YONGXIN OPTICS) to observe and count the cells. Experiments were conducted in triplicate and repeated three times.

2.8 Migration Assessment (Wound Healing Assay)

Horizontal lines were drawn on the back of 6-well plates with a marker pen. HTR-8-SVneo cells (5×10^5) were seeded and cultured overnight to reach confluence. The following day, a sterilized 20 μ L pipette tip was used to scratch perpendicular to the pre-drawn lines. After three washes with PBS, we carefully removed any scratched cells from the medium and replaced them with fresh serum-free culture mediums. Subsequently, HTR-8-SVneo cells were cultured for 48 h at 37 °C in 5% CO₂ incubator and imaged under a microscope (YONGXIN OPTICS). The dis-

tance between cells at 0 h and 48 h was calculated using Image J software. Experiments were conducted in triplicate and repeated three times.

2.9 Flow Cytometry Assay

Cell apoptosis was assessed using an Annexin V-/Propidium Iodide (PI) Apoptosis Detection kit (cat.no. KTA0002; Abbkine Scientific). HTR-8-SVneo cells were trypsinized, washed three times with PBS, and resuspended in $1 \times$ Annexin V binding buffer containing Fluorescein Isothiocyanate (FITC)-Annexin V ($5 \mu\text{L}$). Afterward, they were further incubated with PI ($5 \mu\text{L}$) for 15 min in the dark. The stained cells were analyzed using a flow cytometer (BD Bioscience, San Jose, CA, USA), and the data were processed with Kaluza analysis software (version 2.4; Beckman Coulter, Indianapolis, IN, USA). Experiments were conducted in triplicate and repeated three times.

2.10 ROS Production Measurement

ROS levels in HTR-8-SVneo cells were measured using a ROS assay Kit (Beyotime, Shanghai, China). Briefly, HTR-8-SVneo cells (1×10^6) were incubated with 2',7'-dichlorodihydrofluorescein diacetate (DCFH-DA) for 30 min at 37°C . Following three washes with PBS, the DCF fluorescence was observed utilizing an Olympus fluorescence microscope.

2.11 Terminal Deoxynucleotidyl Transferase Deoxyuridine Triphosphate Nick-End Labeling (TUNEL) Staining

One-step TUNEL Apoptosis Assay Kit (cat.no. KTA2011; Abbkine Scientific) was used to measure the TUNEL-positive cells. HTR-8-SVneo cells were fixed with 4% paraformaldehyde for 15 min and permeabilized with 0.25% Triton-X 100 for 20 min. Then, $50 \mu\text{L}$ of TUNEL reaction agent were added and incubated at 37°C for 1 h. Following washing with PBS, cells were stained with DAPI ($5 \mu\text{g}/\text{mL}$) for 5 min in the dark. Images were captured under a fluorescence microscope (Olympus). Experiments were conducted in triplicate and repeated three times.

2.12 Biochemical Assay

Following the manufacturer's guidelines, malondialdehyde (MDA; cat.no. KTB1050) and superoxide dismutase (SOD; cat.no. KTB1030) concentrations were assessed using kits from Abbkine Scientific. Meanwhile, the levels of IL- 1β (cat.no. KTE6013; Abbkine Scientific), LXA4 (cat.no. CSB-E09689h; CUSABIO, Wuhan, Hubei, China) and TNF- α (cat.no. KTE6032; Abbkine Scientific) were evaluated using enzyme-linked immunosorbent assays. Experiments were conducted in triplicate and repeated three times. Clinical results were performed with five human samples per group.

2.13 Statistical Analysis

Data were presented as mean \pm standard deviation and statistically analyzed with GraphPad Prism 10 software (version 10.4.0, Dotmatics, Boston, MA, USA). All quantitative data were tested for normality using the Shapiro-Wilk test. The data were confirmed to show homogeneity of variance through Levene's test. Student *t*-test and ANOVA (one-way) plus Tukey's post-hoc test were used for comparisons as appropriate. Differences were considered when $p < 0.05$.

3. Results

3.1 IP-10 Expression is Upregulated, While LXA4 Level Is Downregulated in Patients With Preeclampsia

A total of 5 patients with preeclampsia and 5 normal pregnancies were enrolled in this study. As illustrated in Fig. 1A, the preeclampsia group exhibited significantly decreased SOD levels ($p < 0.01$) and increased MDA levels ($p < 0.001$). Meanwhile, a notable decrease in the level of LXA4 was observed in both serum and placental tissues of pregnancies with preeclampsia (Fig. 1B, $p < 0.01$). ALX exhibits high affinity for LXA4 and mediates various cellular effects upon binding [21]. Since LXA4 is not a protein, ALX expression can serve as an indirect indicator of LXA4 activity. Therefore, we further assessed LXA4 production in pregnancies with preeclampsia by analyzing the levels of ALX. As shown in Fig. 1C–E, the mRNA and protein levels of ALX were remarkably reduced in the placental tissues of patients with preeclampsia ($p < 0.05$), whereas the expression levels of IP-10 exhibited the contrasting results ($p < 0.05$). It is well known that IP-10 mediates the migration of immune cells (e.g., T cells and natural killer cells) to inflammatory or infectious sites by binding to its specific receptor, CXCR3 [22]. We further observed that CXCR3 expression levels were markedly upregulated in the preeclampsia group compared to the normal group (Fig. 1E, $p < 0.01$).

3.2 The Antagonistic Relationship Between IP-10 and LXA4 in the Proliferation and Apoptosis of HTR-8-SVneo Cells

We subsequently silenced IP-10 and ALX in hypoxia-induced HTR-8-SVneo cells to investigate their effects on cellular behaviors. IP-10 (Fig. 2A, $p < 0.0001$) and ALX (Fig. 2B, $p < 0.01$) expression were markedly reduced after silencing. si-IP-10-3 and si-ALX-2 were selected for subsequent functional experiments due to their relatively high silencing efficiency ($\geq 60\%$ reduction in mRNA expression compared with the si-NC group). Hypoxia treatment significantly inhibited the viability and colony numbers of HTR-8-SVneo cells (Fig. 2C,D, $p < 0.001$). Notably, IP-10 silencing significantly enhanced the proliferative capacity of HTR-8-SVneo cells (Fig. 2C,D, $p < 0.001$), whereas ALX silencing attenuated this capacity (Fig. 2C,D, $p < 0.01$). The subsequent flow cytometry and TUNEL as-

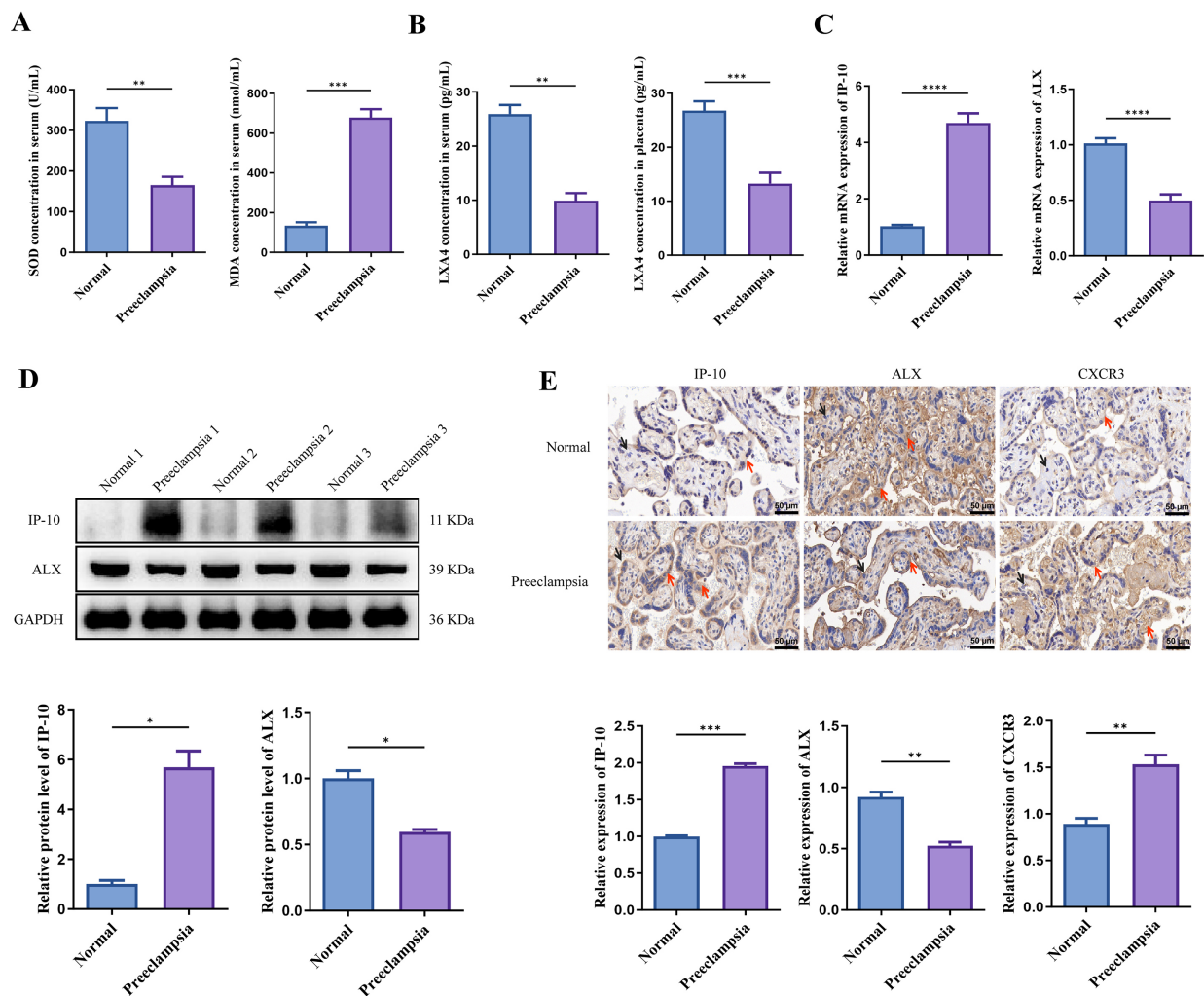


Fig. 1. IP-10 expression is upregulated, while LXA4 level is downregulated in patients with preeclampsia. (A,B) SOD and MDA levels as well as LXA4 concentration in patients with preeclampsia were measured via biochemical assay. (C) The mRNA expression of IP-10 and ALX in patients with preeclampsia was examined via qRT-PCR. (D,E) The protein levels of IP-10, ALX and/or CXCR3 in patients with preeclampsia were measured by western blot and immunohistochemistry. Scale bar = 50 μ m. The hematoxylin-stained nuclei appear blue (black arrow), and the positive DAB staining is characterized by a brown color (red arrow). * $p < 0.05$, ** $p < 0.01$, *** $p < 0.001$, **** $p < 0.0001$. For qRT-PCR and biochemical assay, the results were performed with five human samples per group. For western blot and immunohistochemistry, the results were performed with three human samples per group. Student's *t*-test was used for comparison. SOD, superoxide dismutase; MDA, malondialdehyde; qRT-PCR, quantitative real-time polymerase chain reaction; CXCR3, Cys-X-Cys motif chemokine receptor 3; DAB, 3,3'-diaminobenzidine.

says showed that silencing of IP-10 exhibited a markedly inhibiting effect on HTR-8-SVneo cell apoptosis (Fig. 2E,F, $p < 0.01$), while silencing of ALX showed the opposite results (Fig. 2E,F, $p < 0.05$). This finding was further confirmed by qRT-PCR and western blot assays. We observed that following transfection of si-IP-10, Bcl-2 expression level was upregulated (Fig. 2G,H, $p < 0.05$), and the expression levels of Caspase-3 and Bax were downregulated (Fig. 2G,H, $p < 0.05$). Concurrently, silencing of ALX exerted the opposite influences on these proteins (Fig. 2G,H, $p < 0.05$). Furthermore, ALX silencing significantly increased IP-10 levels (Fig. 2G,H, $p < 0.001$), and IP-10 silencing promoted ALX expression (Fig. 2G,H, $p < 0.05$).

Notably, LXA4 concentration in hypoxia-induced HTR-8-SVneo cells was elevated upon transfection of si-IP-10 (Fig. 2I, $p < 0.01$), but was inhibited upon si-ALX transfection (Fig. 2I, $p < 0.01$). Notably, co-treatment experiments (Fig. 2C-H) showed that ALX silencing significantly reversed the pro-proliferative effect of IP-10 knockdown ($p < 0.001$), and partially attenuated its anti-apoptotic effect ($p < 0.01$). In contrast, silencing of IP-10 remarkably attenuated the inhibiting effects of ALX knocking down on proliferation ($p < 0.01$), and reversed the promoting effects on apoptosis ($p < 0.05$). These results suggested the antagonistic relationship of IP-10 and LXA4 in hypoxia-induced HTR-8-SVneo cells.

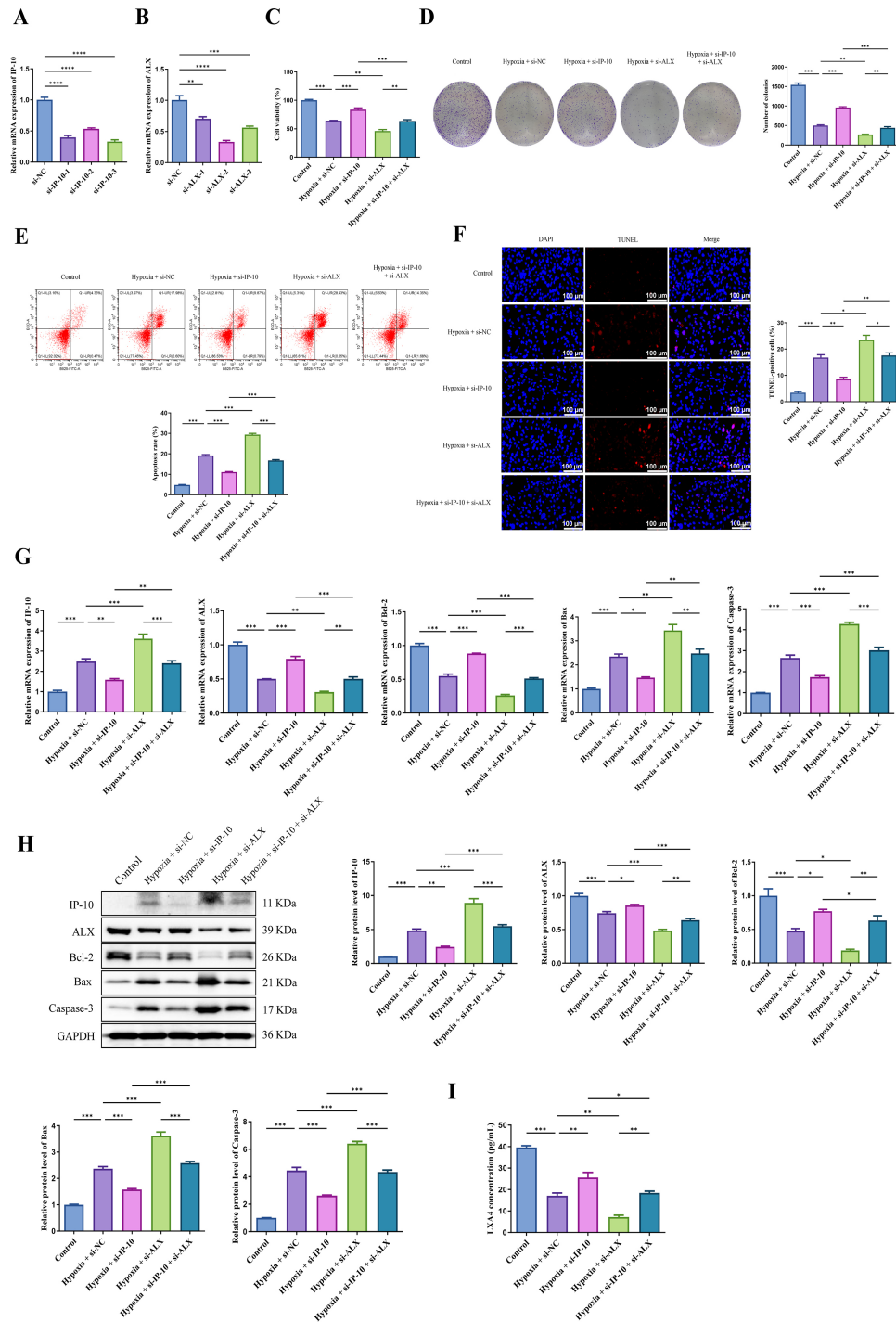


Fig. 2. The antagonistic relationship between IP-10 and LXA4 in the proliferation and apoptosis of hypoxia-induced HTR-8-SVneo cells. (A) IP-10 mRNA expression in hypoxia-induced HTR-8-SVneo cells after transfection of si-IP-10-1/-2/-3 or si-NC. (B) ALX mRNA expression in hypoxia-induced HTR-8-SVneo cells after transfection of si-ALX-1/-2/-3 or si-NC. (C,D) Following transfection, HTR-8-SVneo cell proliferation was assessed by CCK-8 and colony formation assays. (E,F) Flow cytometer and TUNEL staining were conducted to measure the apoptosis of HTR-8-SVneo cells. Scale bar = 100 μ m. (G) The mRNA expression of IP-10, ALX, Bcl-2, Bax and Caspase-3 in hypoxia-induced HTR-8-SVneo cells was detected via qRT-PCR. (H) The protein levels of IP-10, ALX, Bcl-2, Bax and Caspase-3 in hypoxia-induced HTR-8-SVneo cells were measured by western blot. (I) LXA4 concentrations in hypoxia-induced HTR-8-SVneo cells were measured via biochemical assay. * $p < 0.05$, ** $p < 0.01$, *** $p < 0.001$, **** $p < 0.0001$. Experiments were conducted in triplicate and repeated three times. ANOVA (one-way) plus Tukey's post-hoc test was used for comparison. CCK-8, cell counting kit-8; TUNEL, terminal deoxynucleotidyl transferase deoxyuridine triphosphate nick-end labeling.

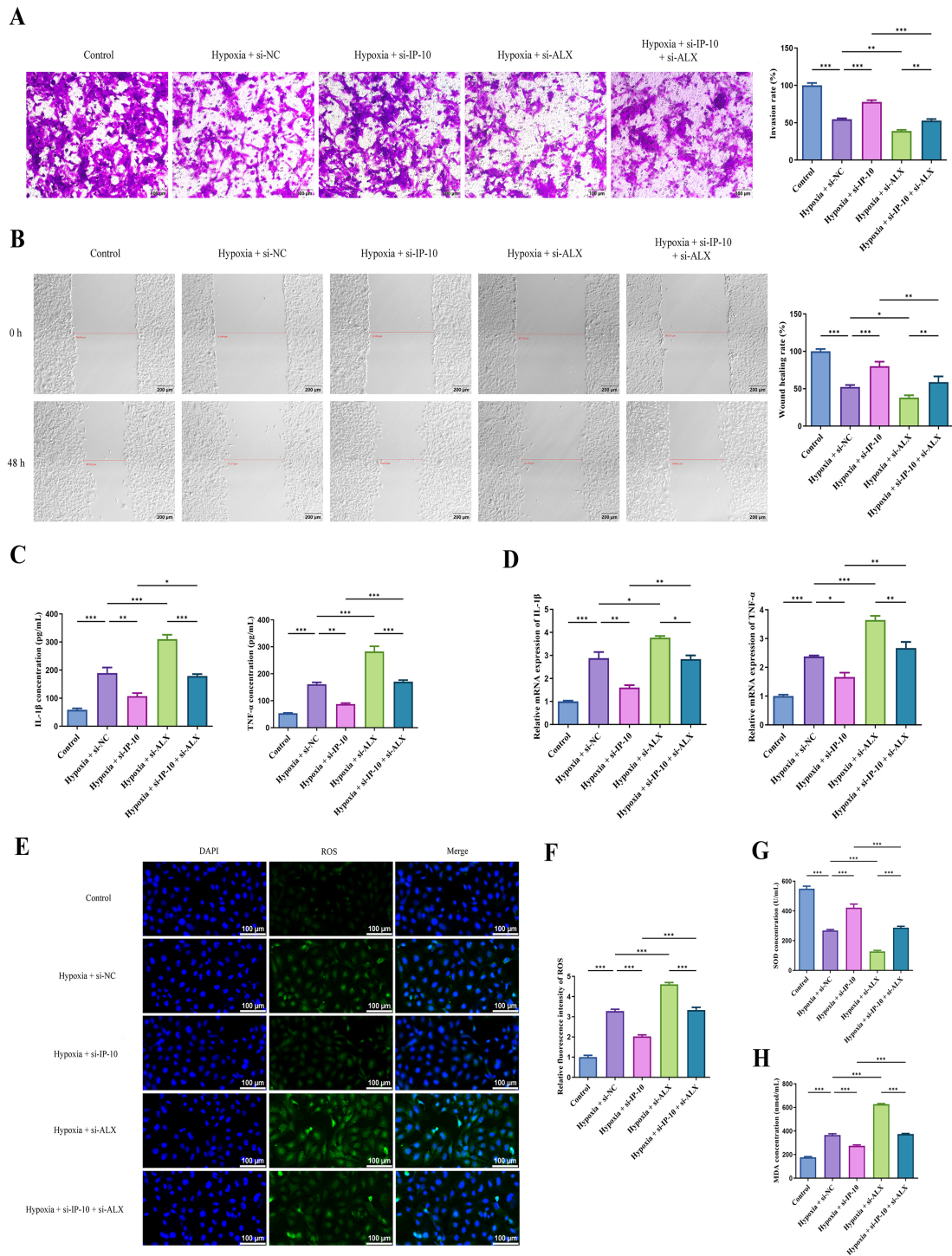


Fig. 3. The antagonistic relationship between IP-10 and LXA4 in the invasion, migration, oxidative stress and inflammation of HTR-8-Svneo cells. (A,B) The invasion (scale bar = 100 μm) and migration (scale bar = 200 μm) of HTR-8-SVneo cells were evaluated through transwell and wound healing assays. (C,D) The concentrations and mRNA expression of IL-1 β and TNF- α in hypoxia-induced HTR-8-SVneo cells were measured by ELISA and qRT-PCR. (E,F) ROS generation was calculated by DCFH-DA staining in hypoxia-induced HTR-8-SVneo cells. Scale bar = 100 μm . (G,H) The concentrations of SOD and MDA in hypoxia-induced HTR-8-SVneo cells were measured by biochemical assay. * $p < 0.05$, ** $p < 0.01$, *** $p < 0.001$. Experiments were conducted in triplicate and repeated three times. ANOVA (one-way) plus Tukey's post-hoc test was used for comparison. MDA, malondialdehyde; ROS, reactive oxygen species; ELISA, enzyme-linked immunosorbent assay; DCFH-DA, 2',7'-dichlorodihydrofluorescein diacetate.

3.3 The Antagonistic Relationship Between IP-10 and LXA4 in the Invasion, Migration, Oxidative Stress and Inflammation of HTR-8-SVneo Cells

Subsequently, the effects of IP-10 and LXA4 on the invasion, migration, oxidative stress and inflammation of HTR-8-SVneo cells were further determined. si-IP-10 transfection significantly enhanced the invasion and migration of HTR-8-SVneo cells (Fig. 3A,B, $p < 0.001$). Conversely, ALX silencing significantly inhibited these biological behaviors (Fig. 3A,B, $p < 0.05$). Furthermore, we indicated that the concentrations of IL-1 β and TNF- α in HTR-8-SVneo cells were significantly reduced following transfection with si-IP-10 (Fig. 3C, $p < 0.01$). In contrast, these indicators exhibited a notable increase when ALX was silenced (Fig. 3C, $p < 0.001$). A similar trend was observed in the mRNA expression of IL-1 β and TNF- α (Fig. 3D, $p < 0.05$). Additionally, as illustrated in Fig. 3E–H, si-IP-10 transfection in hypoxia-induced HTR-8-SVneo cells resulted in lower ROS and MDA levels, and higher SOD activity ($p < 0.001$), while si-ALX transfection exerted the opposite effects on these oxidative stress indicators. As illustrated in Fig. 3A–H, we found that silencing of ALX significantly reversed the promoting effects of IP-10 knock down on cell invasion and migration ($p < 0.01$), while concurrently partially attenuating the inhibiting effects on oxidative stress and inflammation ($p < 0.05$). Conversely, silencing of IP-10 remarkably attenuated the inhibiting effects of ALX knocking down on cell invasion and migration ($p < 0.01$), and reversed the promoting effects on oxidative stress and inflammation ($p < 0.05$).

4. Discussion

The prevalence of preeclampsia in China ranges from 2.4% to 4.2%, with a higher burden in economically underdeveloped regions where preventive and therapeutic resources are limited [23]. Currently, the most effective strategy for the management of preeclampsia remains pregnancy termination and placental delivery. However, determining the optimal timing for delivery remains a challenging study [24]. While studies indicate that fish oil, vitamin D, and aspirin may play key roles in the prevention of preeclampsia, conclusive scientific evidence supporting their efficacy is still lacking [25,26]. Furthermore, the healthcare burden of preeclampsia is substantial, with average maternal and infant medical costs reaching \$41,790 [27]. Consequently, there is an urgent need to identify novel molecular targets for the diagnosis and treatment of preeclampsia in pregnant individuals. In this study, IP-10 and LXA4 were confirmed to exhibit antagonistic effects on the proliferation, migration, and invasion of HTR-8-SVneo cells.

Preeclamptic patients showed characteristic expression patterns in serum and placental tissues: elevated IP-10 levels and reduced LXA4 (and its receptor ALX) levels. Compared with single biomarkers, the combined detection

of serum IP-10 and LXA4 can improve diagnostic accuracy, especially for early screening in the second trimester. Since serum samples are obtained through minimally invasive procedures, this combined biomarker panel is feasible for routine prenatal screening, even in resource-limited settings. Future studies with larger cohorts are needed to validate threshold values for IP-10 and LXA4 that distinguish preeclamptic from normal pregnancies, and to assess their predictive value for early-onset or severe preeclampsia.

Numerous studies have reported that elevated IP-10 levels may act as a pathogenic factor in cancer development [28–30]. These findings collectively indicate that IP-10 may serve as a promising therapeutic target for cancer treatment. Given the shared importance of cell proliferation and invasion in both cancer pathogenesis and preeclampsia development, we hypothesized that abnormal IP-10 levels may also be associated with preeclampsia development. In this study, significantly upregulated expression levels of IP-10 were observed in placental tissues of patients with preeclampsia. This finding aligns with the conclusions of previous study [22], further validating the pathogenic role of IP-10 in preeclampsia progression. Notably, a seemingly paradoxical finding emerged when comparing IP-10's function in cancer and trophoblast cells: knocking down IP-10 effectively promoted the metastasis and growth of HTR-8-SVneo cells and inhibited their apoptosis, while silencing of IP-10 typically exerts anti-tumor effects in cancer development, such as inhibiting cancer cell proliferation and migration. This discrepancy stems from fundamental differences in the regulatory mechanisms governing cell proliferation and migration in cancer cells versus trophoblast cells. Cancer cells exhibit unregulated, dysplastic proliferation and invasion driven by disrupted signaling networks, where IP-10 may act as an “oncogenic driver” by activating pathways such as CXCR3-NF- κ B to enhance malignant behaviors [31,32]. In contrast, trophoblast cells require tightly controlled, directional proliferation and migration to support spiral artery remodeling and placental development. As a chemokine, IP-10 does not promote unbridled trophoblast expansion; instead, it likely acts as a “migration guide” via tissue-specific signaling crosstalk (e.g., interactions with integrin α v β 3 or the decoy receptor ACKR3). This regulation ensures trophoblasts invade the uterine wall to an appropriate depth—neither insufficiently nor excessively [33]. Thus, we suggest that IP-10's function shifts from “progressive” in cancers to “regulatory” in trophoblasts, reflecting a context-dependent role shaped by cell type and microenvironmental cues.

In contrast to IP-10's pathogenic role, LXA4 activation has been shown to exert anti-cancer effects [34,35]. Building on these findings, we hypothesized that LXA4 may exert effects antagonistic to IP-10 in preeclampsia. Given that LXA4 is a non-protein mediator and ALX is its primary receptor, we used ALX expression as an indirect surrogate for LXA4 activity. In this study, we indi-

cated that the deficiency of ALX markedly induced HTR-8-SVneo cell apoptosis, while concurrently suppressing the metastasis and growth. These findings supported our hypothesis. Meanwhile, numerous studies have illustrated the inhibitory effects of LXA4 overexpression on the progression of preeclampsia [36,37], thereby further corroborating our experimental results. Oxidative stress and inflammation are well-recognized pathogenic factors in preeclampsia [38,39]. Our data showed that IP-10 and LXA4 also exert opposing regulatory effects on these processes. Specifically, silencing IP-10 inhibited oxidative stress and inflammation, while knocking down LXA4 increased both. Collectively, these results confirmed that IP-10 and LXA4 exhibit antagonistic roles in regulating HTR-8-Svneo cell proliferation, migration, and invasion, as well as oxidative stress and inflammation, during preeclampsia progression.

Limitations

This study has several notable limitations that should be acknowledged. First, as a pilot study, this research enrolled only 5 patients per group. The small sample size may limit the generalizability of our clinical findings, and larger cohorts are needed in future studies to validate these results. Second, the regulatory mechanisms of IP-10 and LXA4 in HTR-8-Svneo cells—including potential downstream signaling pathways—remain to be fully elucidated. For example, IP-10 activates NF- κ B signaling pathway by binding to CXCR3, while NF- κ B pathway serves as the core regulatory mechanism for the transcription of IL-1 β and TNF- α [12]. The interactions among IP-10, CXCR3, LXA4 and NF- κ B pathway in preeclampsia may be a valuable focus for future research. Meanwhile, IP-10 mediates immune cell migration to inflammatory sites by targeting CXCR3 [22]. Further exploring whether IP-10 knockdown reduces maternal pro-inflammatory cytokine levels and modulates immune cell polarization would enhance the rigor of our findings. Third, additional experimental data on oxidative stress and inflammation are needed. Additionally, cell line studies also have inherent limitations in recapitulating clinical outcomes. This study only conducted preliminary research at the cellular level, and lacked validation of biological integrity, *in vivo* microenvironment, and feasibility of transformation. Their roles in animal models also warrant further investigation. Last but not least, HTR-8-SVneo is an immortalized cell line that may not accurately represent the behaviors of primary trophoblasts. Compared to primary trophoblasts, HTR-8-SVneo cells have limitations including: (i) phenotypic alterations induced by immortalization, which modify cell cycle regulation and apoptosis sensitivity; and (ii) limitations of functional features. The core functions of primary trophoblasts, such as spiral artery remodeling and immune tolerance regulation, rely on complex intercellular communication and microenvironment response, while HTR-8-Svneo cells may lose some key functions during long-term passage. We consider vali-

dating our findings in primary trophoblast cultures and animal models in future work.

5. Conclusions

In a word, this pilot study presents preliminary findings. We have preliminarily characterized the antagonistic effects of IP-10 and LXA4 on HTR-8-SVneo trophoblast cells during preeclampsia progression using *in vitro* models. Our *in vitro* data may provide theoretical support for future animal model experiments and clinical data analysis.

Availability of Data and Materials

The data are available from the corresponding author on reasonable request.

Author Contributions

JW made substantial contributions to the conception and design of the work. JW, CF, LQ and YZ made substantial contributions to the acquisition, analysis and interpretation of data for the work. JW drafted the manuscript. All authors contributed to editorial changes in the manuscript. All authors read and approved the final manuscript. All authors have participated sufficiently in the work and agreed to be accountable for all aspects of the work.

Ethics Approval and Consent to Participate

Ethical approvals were granted by the Ethics Committee of Jinhua People's Hospital (approval number: 2023-007), and this study complies with the principles set forth in the Declaration of Helsinki. All participants gave their written informed consent.

Acknowledgment

Not applicable.

Funding

This work was supported by Key Science and Technology Projects of Jinhua City in 2023 (Project No: 2023-3-137).

Conflict of Interest

The authors declare no conflict of interest.

References

- [1] MacDonald TM, Walker SP, Hannan NJ, Tong S, Kaitu'u-Lino TJ. Clinical tools and biomarkers to predict preeclampsia. *eBioMedicine*. 2022; 75: 103780. <https://doi.org/10.1016/j.ebiom.2021.103780>.
- [2] de Moreuil C, Hannigsberg J, Chauvet J, Remoue A, Tremouilhac C, Merviel P, *et al*. Factors associated with poor fetal outcome in placental abruption. *Pregnancy Hypertension*. 2021; 23: 59–65. <https://doi.org/10.1016/j.preghy.2020.11.004>.
- [3] Kasuya M, Akiba N, Iriyama T, Sayama S, Kubota K, Toshimitsu M, *et al*. The impact of fetal growth restriction in diagnosing preeclampsia on the severity of maternal features. *The Journal*

- of Obstetrics and Gynaecology Research. 2022; 48: 912–919. <https://doi.org/10.1111/jog.15152>.
- [4] Jung E, Romero R, Yeo L, Gomez-Lopez N, Chaemsaihong P, Jaovisidha A, *et al.* The etiology of preeclampsia. *American Journal of Obstetrics and Gynecology*. 2022; 226: S844–S866. <https://doi.org/10.1016/j.ajog.2021.11.1356>.
- [5] Varberg KM, Soares MJ. Paradigms for investigating invasive trophoblast cell development and contributions to uterine spiral artery remodeling. *Placenta*. 2021; 113: 48–56. <https://doi.org/10.1016/j.placenta.2021.04.012>.
- [6] Korbecki J, Kojder K, Kapczuk P, Kupnicka P, Gawrońska-Szklarz B, Gutowska I, *et al.* The Effect of Hypoxia on the Expression of CXC Chemokines and CXC Chemokine Receptors—A Review of Literature. *International Journal of Molecular Sciences*. 2021; 22: 843. <https://doi.org/10.3390/ijms22020843>.
- [7] Zhao Y, Yang X, Zhang X, Yu Q, Zhao P, Wang J, *et al.* IP-10 and RANTES as biomarkers for pulmonary tuberculosis diagnosis and monitoring. *Tuberculosis (Edinburgh, Scotland)*. 2018; 111: 45–53. <https://doi.org/10.1016/j.tube.2018.05.004>.
- [8] Torres-Vázquez J, Uriel Vázquez-Medina M, Comoto-Santacruz DA, Pradillo-Macias ME, Muñoz-Monroy OE, Martínez-Cuazitl A. Relationship of IP-10 gene expression to systemic lupus erythematosus activity. *Reumatologia Clinica*. 2022; 18: 91–93. <https://doi.org/10.1016/j.reumae.2021.01.001>.
- [9] Makarem YS, Ahmed EA, Makboul M, Farghaly S, Mostafa N, El Zohne RA, *et al.* CXCL10 as a biomarker of interstitial lung disease in patients with rheumatoid arthritis. *Reumatologia Clinica*. 2024; 20: 1–7. <https://doi.org/10.1016/j.reumae.2023.12.005>.
- [10] Zhou Y, Wang S, Ma JW, Lei Z, Zhu HF, Lei P, *et al.* Hepatitis B virus protein X-induced expression of the CXC chemokine IP-10 is mediated through activation of NF- κ B and increases migration of leukocytes. *The Journal of biological chemistry*. 2010; 285: 12159–12168. <https://doi.org/10.1074/jbc.M109.067629>.
- [11] Dîjmărescu AL, Boldeanu L, Radu M, Rotaru I, Siminel MA, Manolea MM, *et al.* The potential value of diagnostic and predictive serum biomarkers for preeclampsia. *Romanian Journal of Morphology and Embryology = Revue Roumaine De Morphologie et Embryologie*. 2021; 62: 981–989. <https://doi.org/10.47162/RJME.62.4.10>.
- [12] Darakhshan S, Hassanshahi G, Mofidifar Z, Soltani B, Karimabad MN. CXCL9/CXCL10 angiostasis CXC-chemokines in parallel with the CXCL12 as an angiogenesis CXC-chemokine are variously expressed in pre-eclamptic-women and their neonates. *Pregnancy Hypertension*. 2019; 17: 36–42. <https://doi.org/10.1016/j.preghy.2019.05.001>.
- [13] McGuffee RM, Luetzen MA, Ford DA. Resolving lipoxin A₄: Endogenous mediator or exogenous anti-inflammatory agent? *Journal of Lipid Research*. 2025; 66: 100734. <https://doi.org/10.1016/j.jlr.2024.100734>.
- [14] Pan WH, Hu X, Chen B, Xu QC, Mei HX. The Effect and Mechanism of Lipoxin A₄ on Neutrophil Function in LPS-Induced Lung Injury. *Inflammation*. 2022; 45: 1950–1967. <https://doi.org/10.1007/s10753-022-01666-5>.
- [15] Li Y, Wang N, Ma Z, Wang Y, Yuan Y, Zhong Z, *et al.* Lipoxin A₄ protects against paraquat induced acute lung injury by inhibiting the TLR4/MyD88 mediated activation of the NF- κ B and PI3K/AKT pathways. *International Journal of Molecular Medicine*. 2021; 47: 86. <https://doi.org/10.3892/ijmm.2021.4919>.
- [16] Lin F, Zeng P, Xu Z, Ye D, Yu X, Wang N, *et al.* Treatment of Lipoxin A (4) and its analogue on low-dose endotoxin induced preeclampsia in rat and possible mechanisms. *Reproductive Toxicology (Elmsford, N.Y.)*. 2012; 34: 677–685. <https://doi.org/10.1016/j.reprotox.2012.09.009>.
- [17] Qu H, Yu Q, Jia B, Zhou W, Zhang Y, Mu L. HIF 3 α affects preeclampsia development by regulating EVT growth via activation of the Flt 1/JAK/STAT signaling pathway in hypoxia. *Molecular Medicine Reports*. 2021; 23: 68. <https://doi.org/10.3892/mmr.2020.11701>.
- [18] Liu Z, Liu H, Wang C, Pei J, Chu N, Peng T, *et al.* Identification of LncRNA-miRNA-mRNA ceRNA network in hypoxia-induced HTR-8/SVneo cells for preeclampsia. *Medicine*. 2023; 102: e33649. <https://doi.org/10.1097/MD.00000000000033649>.
- [19] Gaudin A, Tolar M, Peters OA. Lipoxin A₄ Attenuates the Inflammatory Response in Stem Cells of the Apical Papilla via ALX/FPR2. *Scientific Reports*. 2018; 8: 8921. <https://doi.org/10.1038/s41598-018-27194-7>.
- [20] Jiang Y, Huang F, Chai X, Yuan W, Ding H, Wu X. The role of IP-10 and its receptor CXCR3 in early pregnancy. *Molecular Immunology*. 2021; 140: 59–69. <https://doi.org/10.1016/j.molimm.2021.09.013>.
- [21] Gong X, Li J, Jiang Y, Yuan P, Chen L, Yang Y, *et al.* Risk of preeclampsia by gestational weight gain in women with varied prepregnancy BMI: A retrospective cohort study. *Frontiers in Endocrinology*. 2022; 13: 967102. <https://doi.org/10.3389/fendo.2022.967102>.
- [22] Sharma DD, Chandresh NR, Javed A, Girgis P, Zeeshan M, Fatima SS, *et al.* The Management of Preeclampsia: A Comprehensive Review of Current Practices and Future Directions. *Cureus*. 2024; 16: e51512. <https://doi.org/10.7759/cureus.51512>.
- [23] Ushida T, Tano S, Matsuo S, Fuma K, Imai K, Kajiyama H, *et al.* Dietary supplements and prevention of preeclampsia. *Hypertension Research: Official Journal of the Japanese Society of Hypertension*. 2025; 48: 1444–1457. <https://doi.org/10.1038/s41440-025-02144-9>.
- [24] Giourga C, Papadopoulou SK, Voulgaridou G, Karastogiannidou C, Giaginis C, Pritsa A. Vitamin D Deficiency as a Risk Factor of Preeclampsia during Pregnancy. *Diseases (Basel, Switzerland)*. 2023; 11: 158. <https://doi.org/10.3390/diseases11040158>.
- [25] Hao J, Hassen D, Hao Q, Graham J, Paglia MJ, Brown J, *et al.* Maternal and Infant Health Care Costs Related to Preeclampsia. *Obstetrics and Gynecology*. 2019; 134: 1227–1233. <https://doi.org/10.1097/AOG.0000000000003581>.
- [26] Chang C, Wang MJ, Bi XF, Fan ZY, Feng D, Cai HQ, *et al.* Elevated serum eotaxin and IP-10 levels as potential biomarkers for the detection of esophageal squamous cell carcinoma. *Journal of Clinical Laboratory Analysis*. 2021; 35: e23904. <https://doi.org/10.1002/jcla.23904>.
- [27] Clark AM, Heusey HL, Griffith LG, Lauffenburger DA, Wells A. IP-10 (CXCL10) Can Trigger Emergence of Dormant Breast Cancer Cells in a Metastatic Liver Microenvironment. *Frontiers in Oncology*. 2021; 11: 676135. <https://doi.org/10.3389/fonc.2021.676135>.
- [28] Kim M, Choi HY, Woo JW, Chung YR, Park SY. Role of CXCL10 in the progression of in situ to invasive carcinoma of the breast. *Scientific Reports*. 2021; 11: 18007. <https://doi.org/10.1038/s41598-021-97390-5>.
- [29] Wang Z, Ao X, Shen Z, Ao L, Wu X, Pu C, *et al.* TNF- α augments CXCL10/CXCR3 axis activity to induce Epithelial-Mesenchymal Transition in colon cancer cell. *International Journal of Biological Sciences*. 2021; 17: 2683–2702. <https://doi.org/10.7150/ijbs.61350>.
- [30] Yao W, Cui X, Peng H, Zhang Y, Jia X, Wu S, *et al.* IDO1 facilitates esophageal carcinoma progression by driving the direct binding of NF- κ B and CXCL10. *Cell Death Discovery*. 2023; 9: 403. <https://doi.org/10.1038/s41420-023-01689-3>.
- [31] Chevigné A, Janji B, Meyrath M, Reynders N, D’Uonno G, Uchański T, *et al.* CXCL10 Is an Agonist of the CC Family Chemokine Scavenger Receptor ACKR2/D6. *Cancers*. 2021;

- 13: 1054. <https://doi.org/10.3390/cancers13051054>.
- [32] Liu H, Zeng J, Huang W, Xu Q, Ye D, Sun R, *et al.* Colorectal Cancer Is Associated with a Deficiency of Lipoxin A₄, an Endogenous Anti-inflammatory Mediator. *Journal of Cancer*. 2019; 10: 4719–4730. <https://doi.org/10.7150/jca.32456>.
- [33] Xu F, Zhou X, Hao J, Dai H, Zhang J, He Y, *et al.* Lipoxin A₄ and its analog suppress hepatocarcinoma cell epithelial-mesenchymal transition, migration and metastasis via regulating integrin-linked kinase axis. *Prostaglandins & Other Lipid Mediators*. 2018; 137: 9–19. <https://doi.org/10.1016/j.prostaglandins.2018.05.007>.
- [34] Liu H, Cheng F, Xu Q, Huang W, Wang S, Sun R, *et al.* Lipoxin A₄ suppresses angiotensin II type 1 receptor autoantibody in preeclampsia via modulating caspase-1. *Cell Death & Disease*. 2020; 11: 78. <https://doi.org/10.1038/s41419-020-2281-y>.
- [35] Liu H, Huang W, Chen L, Xu Q, Ye D, Zhang D. Glucocorticoid Exposure Induces Preeclampsia *via* Dampening Lipoxin A₄, an Endogenous Anti-Inflammatory and Proresolving Mediator. *Frontiers in Pharmacology*. 2020; 11: 1131. <https://doi.org/10.3389/fphar.2020.01131>.
- [36] Barron A, McCarthy CM, O’Keeffe GW. Preeclampsia and Neurodevelopmental Outcomes: Potential Pathogenic Roles for Inflammation and Oxidative Stress? *Molecular Neurobiology*. 2021; 58: 2734–2756. <https://doi.org/10.1007/s12035-021-02290-4>.
- [37] Negre-Salvayre A, Swiader A, Salvayre R, Guerby P. Oxidative stress, lipid peroxidation and premature placental senescence in preeclampsia. *Archives of Biochemistry and Biophysics*. 2022; 730: 109416. <https://doi.org/10.1016/j.abb.2022.109416>.